

# Temperature Dependence of Mechanical and Dielectric Relaxation in *cis*-1,4-Polyisoprene

P. G. Santangelo and C. M. Roland\*

Chemistry Division, Code 6120, Naval Research Laboratory, Washington, D.C. 20375-5342

Received November 12, 1997; Revised Manuscript Received March 9, 1998

**ABSTRACT:** The linear viscoelastic properties of 1,4-polyisoprene (PI;  $M_w = 504\,000$ ) were measured by combined mechanical and dielectric spectroscopies. For local segmental motion, the respective mechanical and dielectric relaxation times, although differing substantially in magnitude, have identical temperature dependencies. The shape of the segmental relaxation function itself was sensitive to temperature. The data, obtained over a 160 degree range of temperatures, could be reduced to yield ostensibly satisfactory master curves; however, detailed analysis reveals the usual breakdown of time–temperature superpositioning in the glass transition zone. Given the near equivalence of the respective breadths of its terminal and segmental dispersions, thermorheological complexity in PI is unanticipated by theory. In the plateau zone, the mechanical spectrum of PI exhibits power law behavior, with an exponent (0.21) close to a proposed universal value.

## Introduction

The low-frequency motion of entangled, flexible-chain polymers can be described with some success by the reptation model,<sup>1–3</sup> wherein the actual chain is represented as a Rouse chain confined to a tube. At shorter times, the chain segments move freely within the tube, so that the relevant relaxation times are just those of the Rouse model.<sup>2,4,5</sup> These relaxation times can be expressed in terms of the characteristic relaxation time,  $\tau_0$ , of a Rouse unit where, enumerating only the tem-

$$\tau_0 \propto \frac{\zeta}{T} \quad (1)$$

perature-dependent quantities,  $\zeta$  is the local friction coefficient and  $T$  is temperature. Rouse relaxation proceeds until constrained by the entanglements. The longest Rouse relaxation time, corresponding to longitudinal fluctuations of the chain within a tube, depends quadratically on molecular weight and is directly proportional to  $\tau_0$ .<sup>2</sup>

The slowest dynamics is governed by one-dimensional diffusion of the chain from the tube, the rate of which depends both on molecular weight and the entanglement concentration. This reptation time is directly proportional to  $\tau_0$ , so that all temperature-dependent quantities are contained in eq 1.<sup>1,2</sup>

Thus, according to the reptation model, the only temperature-dependent quantity (other than the weak  $T^{-1}$  scaling) is  $\zeta$ , which is just the Rouse friction coefficient. The parameter  $\zeta$  can be evaluated from the flow viscosity of unentangled polymers ( $\eta \propto \zeta$ ),<sup>6</sup> or from the moduli at the high-frequency end of the glass transition zone [at frequencies  $\omega$  for which  $G'(\omega) = G''(\omega) \propto (\zeta \omega)^{1/2}$ ].<sup>5</sup> Thus, the  $\zeta$  of reptation theory is identified with the friction coefficient prevailing both in the flow regime (involving chain modes) and at onset of glassy behavior (i.e., segmental relaxation). For this reason reptation theory can be said to *predict* thermorheological simplicity in polymers.<sup>7</sup>

Since its discovery in the early 1950s, the principle of time–temperature superpositioning has enjoyed wide application.<sup>5</sup> Many recent texts,<sup>8–12</sup> as well as review

articles,<sup>7,13</sup> assert the thermorheological simplicity of polymers. Experimentally, however, there is accumulating evidence of departures from the time–temperature superposition principle in polymers, due to a difference in temperature dependency between local segmental relaxation and relaxation of the chain modes. Such thermorheological complexity is most readily observed in the softening zone of the viscoelastic spectrum. Examples include polystyrene,<sup>14</sup> poly(vinyl acetate),<sup>15</sup> polypropylene glycol,<sup>16</sup> poly(phenylmethylsiloxane),<sup>17</sup> polybutadiene,<sup>18</sup> polyisobutylene,<sup>19</sup> and atactic polypropylene.<sup>20,21</sup>

*Cis*-1,4-polyisoprene (PI) is an interesting material, not only because of its enormous commercial significance (natural rubber comprises 35% of all commercial elastomers<sup>22</sup>), but also because it exhibits unusual viscoelastic behavior. For example, although much progress has been made in relating the chemical structure of polymers to the magnitude of their plateau modulus,<sup>23,24</sup> all approaches to this problem over-estimate the plateau modulus of PI, by at least a factor of 2.<sup>25,26</sup>

The effect long-chain branching has on the rheology of PI is also unexplained. The terminal zone of branched polymers is known to broaden with decreasing temperature, an effect ascribed to arm retraction.<sup>27</sup> Various workers have pointed out that, given the relative energies of its *gauche* and *trans* rotamers, for branched PI this broadening effect should be absent. Therefore, PI would represent a unique case among branched polymers of thermorheological simplicity in the terminal zone.<sup>28–31</sup> Contrary to this, recent experiments showed that star-branched PI exhibits a breakdown of time–temperature superpositioning in the terminal zone.<sup>32–34</sup>

Although deviation from time–temperature superpositioning in neat polymers is at odds with the reptation model,<sup>7</sup> the coupling model of relaxation predicts a differing temperature dependence between any relaxation modes that have a different spectral breadth.<sup>35–39</sup> PI is an interesting test case regarding this prediction, because its segmental relaxation dispersion is unusually narrow,<sup>40</sup> and hence the expectation from the coupling model is similar temperature dependencies for its terminal and segmental relaxations.

Dielectric spectroscopy of both the normal and segmental modes in PI have been carried out,<sup>41–43</sup> although conductivity complications severely limit the range over which data can be obtained for PI of molecular weights greater than  $\sim 40\,000$ . Nevertheless, the dielectric data suggest a weaker temperature dependence of the normal mode in comparison to segmental relaxation. Evaluation of the thermorheological behavior of polymers requires data over a broad time scale, so that the segmental and the chain modes are simultaneously observable. This data can be obtained from measurements of the softening zone, although it is still necessary to have a wide range of experimental frequencies. The latter is accomplished by employing more than one form of spectroscopy. Osaki and co-workers<sup>44</sup> have analyzed dynamic birefringence and mechanical measurements on PI. Employing a modified stress optical law, which relies on the assumption of additivity of “rubbery” and “glassy” stresses, they conclude the PI is thermorheologically complex in the glass transition zone. In the present work, segmental relaxation behavior is characterized both mechanically and dielectrically. For the terminal mode, we use mechanical spectroscopy, extending the range of frequencies by analyzing the compliance function in addition to the modulus.

## Experimental Section

The linear PI was synthesized by A. F. Halasa, using *n*-butyllithium as the initiator. It is essentially a copolymer (92% 1,4 microstructure, high cis), and thus completely amorphous. The PI has a molecular weight equal to 504 000, as determined from the zero-shear viscosity,<sup>30</sup> measured with a constant stress rheometer.<sup>45</sup> Dynamic mechanical data was obtained using a Bohlin VOR with a parallel plate geometry. Isothermal measurements were made over a range from  $-71$  (roughly the calorimetric  $T_g$ ) to  $+90$  °C, with  $\pm 0.1$ ° control. The data were reduced empirically to yield apparent master curves. This reduction procedure entails small vertical shifts, partly a consequence of errors in specimen radius. For a parallel plate geometry, the modulus depends on the fourth power of the radius.

Dielectric experiments employed a time domain spectrometer (IMASS Inc.), with the sample contained in a Delta Design Model 9023 oven. The sample was contained between aluminum plates with a guard ring on the detector side. Data were obtained over a temperature range from  $-67$  to  $-37$  °C (temperature stability  $\approx 0.1$ °).

## Results and Discussion

**Terminal Relaxation.** Although a purpose of the present work was to determine if PI is thermorheologically simple, master curves of the dynamic mechanical data were constructed that are at least qualitatively accurate. Measurements obtained at six temperatures are shown in Figure 1. In the terminal zone (ca.  $-6 < \log \omega < 1$  in Figure 1), where  $G''(\omega)$  exhibits a maximum, this time–temperature reduction is readily accomplished because there is sufficient “structure” in the viscoelastic functions. Over the same frequency range, however, the compliance is relatively featureless. Depending on the amount of vertical shifting applied, different frequency shifts could accomplish superpositioning of  $J'(\omega)$  equally well. Toward higher frequencies ( $1 < \log \omega < 7$ ),  $J''(\omega)$  exhibits a peak, and superpositioning of the compliance function becomes accurate. In this regime, however, unique reduction of the monotonic modulus curves is no longer feasible.

Thus, temperature shifts for the chain modes ( $-6 < \log \omega < 7$ ) can be determined over the entire range of

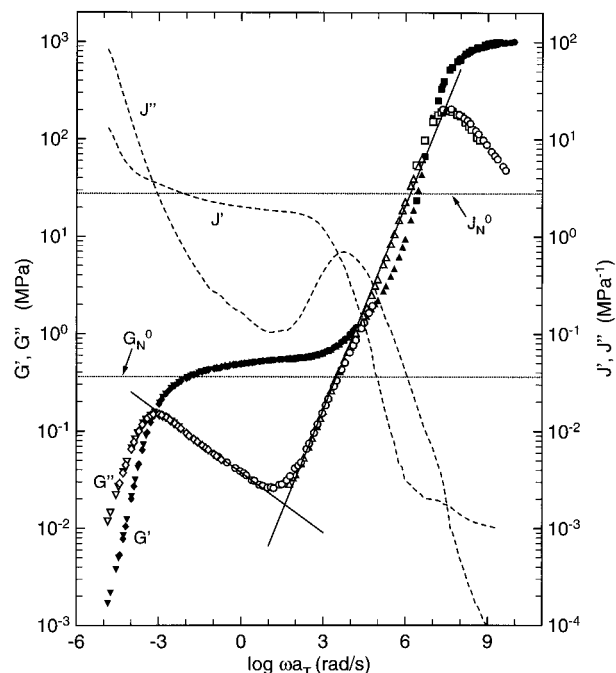


**Figure 1.** Apparent master curves ( $T_{ref} = -10$  °C) for the storage (solid symbols) and loss (hollow symbols) moduli of PI; in the transition zone, the superpositioning is only approximate (see text). Also shown (as dashed lines) are the corresponding dynamic compliances. The value of the plateau modulus is indicated by the horizontal line. The solid lines, having slopes of  $-0.21$  and  $0.70$  respectively, represent fits to  $G'$  in the power law regimes.

frequencies, but only by relying on different viscoelastic functions. To corroborate the quantitative validity of this reduction scheme, it must be shown that the same viscoelastic mechanism is being probed throughout. We do this by evaluating the integrals of the respective  $G''(\omega)$  and  $J'(\omega)$  peaks. The loss modulus peak is related to the plateau modulus characterizing the entanglement density<sup>5</sup> where the upper limit restricts

$$G_N^0 = \frac{2}{\pi} \int_{-\infty}^a G''(\omega) d \ln \omega \quad (2)$$

the integration to the terminal zone. Similarly,  $G_N^0$  can be obtained from the loss compliance peak using<sup>5</sup>

$$G_N^0 = \left[ \frac{2}{\pi} \int_b^{+\infty} J''(\omega) d \ln \omega \right]^{-1} \quad (3)$$

As shown in Figure 2, the terminal mode can be resolved from any overlap of the transition zone by using a power law to approximate the loss modulus on the high-frequency side<sup>46</sup> (and similarly for the low-frequency side of the loss compliance). Carrying out the numerical integration, eqs 2 and 3 yield the same value,  $G_N^0 = 0.36 \pm 0.04$  MPa. This equivalence provides assurance that the time–temperature shifting (for  $\omega < 10$  rad/s) to superimpose the modulus is consistent with the shifting of the compliance data at higher frequencies.

The value of the plateau modulus, which corresponds to a molecular weight between entanglements of 6400 g/mol, agrees with literature values reported previously for PI.<sup>26,47</sup> Determination of the plateau modulus from eq 2 or 3 does not require monodisperse samples, unlike the use of phenomenological relations, for example between the plateau modulus and the maximum in

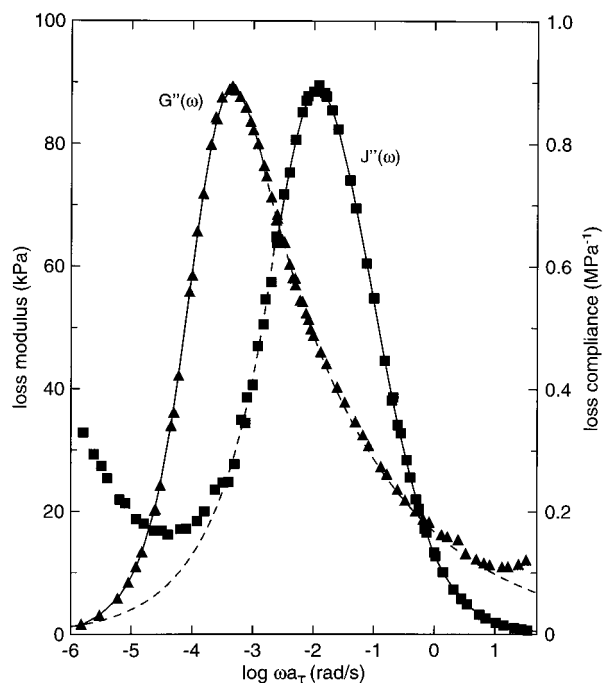


**Figure 2.** Representative terminal dispersions in the loss modulus (▲) and loss compliance (■) at reference temperatures equal to  $-0$  and  $-52$  °C, respectively. The dashed lines represent a power law fit to the spectral wing that is used to remove contributions from the overlapping transition zone. Integration according to eqs 2 and 3 yields  $G_N^0 (= 1/J_N^0) = 0.36$  MPa.

$G'(\omega)$  or  $J'(\omega)$ .<sup>5,48</sup> Multiplying  $G_N^0$  by the maximum in the loss compliance (Figure 1) yields 0.25, which is at the low end of the range of this product found for various linear polymers.<sup>5</sup> As stated earlier, the plateau modulus for PI is substantially less than predicted by various models and correlations.<sup>25,26</sup>

The frequency of the terminal  $G'(\omega)$  maximum is shown in Figure 3 for temperatures in the range  $-10$  to  $90$  °C. The curve represents the Vogel-Fulcher equation<sup>5</sup> with the fit parameters listed in Table 1.

$$\omega_{\max} = A \exp\left(\frac{B}{T - T_{\infty}}\right) \quad (4)$$

Similarly, the frequency of the loss compliance maximum, measured between  $-52$  and  $-40$  °C, is included in Figure 3. Over this temperature range, the two functions represent the same viscoelastic mode, so vertically shift  $\omega_{\max}$  for the compliance (by a factor of  $9.1 \times 10^{-6}$ ), bringing these values into coincidence with the Vogel-Fulcher extrapolation of the modulus data. Such superposition demonstrates the equivalent temperature dependence for the two quantities.

As implied by the extrapolation used in Figure 2, the terminal zone relaxation spectrum of entangled, linear polymers exhibits power law behavior. The exponent,  $n_e$ , can be determined to a good approximation using<sup>49</sup>

$$\lim_{\omega \rightarrow \infty} G'(\omega) \propto \omega^{-n_e} \quad (5)$$

According to reptation theory,  $n_e$  should equal 0.5,<sup>50</sup> but this is not observed experimentally. Recently it has been suggested that, in the high molecular weight limit, a value of  $n_e = 0.23$  is attained for all polymers.<sup>51</sup> Recent work on poly(vinyl methyl ether) of over one

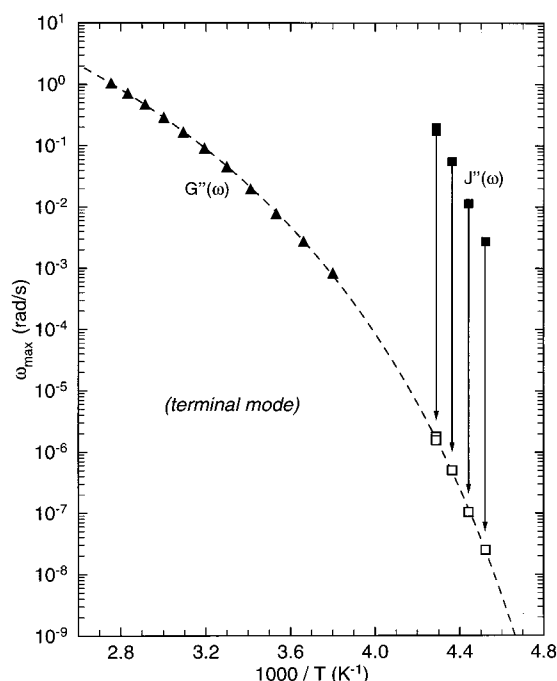


**Figure 3.** The frequency of the terminal dispersion in the loss modulus (▲) and in the loss compliance (■). The respective temperature dependencies are equivalent, as shown by the superposition of the loss compliance data when shifted downward 5.04 decades.

**Table 1. Vogel-Fulcher Parameters (eq 4) for PI**

mode	A	B	$T_{\infty}$	temperature range, °C
terminal	$1.50 \times 10^3$	-1462	162.3	$-52$ to $90$ °C
segmental	$1.47 \times 10^{15}$	-1822	161.7	$-69$ to $-37$ °C

million molecular weight found the exponent to be significantly less than this putative universal value.<sup>52</sup> Because the PI has a molecular weight corresponding to  $>100$  entanglements per chain, we expect the high molecular weight limit to be achieved herein. Fitting the loss modulus data in Figure 1 yields  $n_e = 0.21$ , which is close to the universal value.<sup>51</sup>

There is an expression relating this exponent to the zero shear viscosity<sup>49</sup>

$$\eta_0 = \frac{n_e}{n_e + 1} G_N^0 \lambda_{\max} \quad (6)$$

where  $\lambda_{\max}$ , the longest relaxation time, can be deduced from the frequency,  $\omega_0$ , at which the low-frequency asymptotes of  $G'(\omega)$  and  $G''(\omega)$  would intersect<sup>49</sup>

$$\lambda_{\max} = \frac{n_e + 2}{n_e + 1} \times \omega_0^{-1} \quad (7)$$

This gives  $\lambda_{\max} \sim 10$  s at  $60$  °C. Using  $n_e = 0.21$ , eq 6 predicts  $\eta_0 = 7 \times 10^5$  Pa·s, which is 40% less than the zero-shear viscosity directly measured,  $\eta_0 = 1.2 \times 10^6$  Pa·s. The origin of this discrepancy is not obvious, although polydispersity is likely a contributing factor.<sup>53</sup>

**Segmental Relaxation.** At temperatures in the range of  $-56$  to  $-71$  °C, local segmental relaxation transpires within the range of available frequencies, giving rise to a peak in  $G'(\omega)$  at  $\log \omega \sim 7.5$  in Figure 1. The frequencies corresponding to the maximum are plotted in Figure 4. Whereas the shape of the terminal relaxation function is insensitive to temperature, the seg-

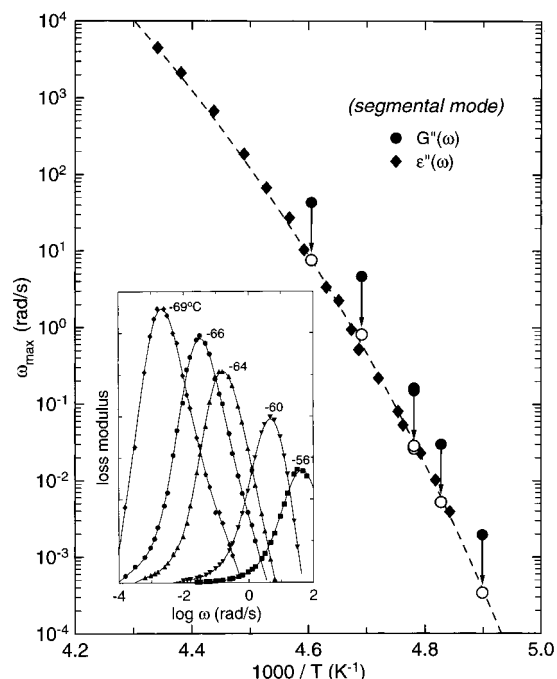


**Figure 4.** The frequency of the segmental relaxation dispersion in the loss modulus (●) and in the dielectric loss (◆). The mechanical data superimpose on the dielectric results when the peak frequencies of the former are multiplied by 0.175. Representative loss modulus peaks are shown in the inset; note the broadening as temperature is reduced.

mental peaks broaden with decreasing temperature (see inset to Figure 4). This trivial departure from time-temperature equivalence was also seen in polybutadiene.<sup>54</sup>

The range of frequencies over which the segmental relaxation time could be determined was extended using dielectric spectroscopy. (Note that in principle the terminal relaxation could also be probed dielectrically, because *cis*-polyisoprene has a dipole moment parallel to the chain contour. However, such measurements are limited to relatively low molecular weight polymers due to interference from conductivity.) The frequency of the maximum in the dielectric loss corresponding to local segmental motion was obtained over the temperature range from  $-67$  to  $-37$  °C. The dielectric  $\omega_{\max}$  are a factor of 5.7 smaller than the values determined mechanically at the same temperature. (This compares to a factor of 2 difference in the respective  $\omega_{\max}$  for high vinyl polybutadiene.<sup>54</sup>) Such differences are in part due to the fact that retardation times are always longer than the corresponding relaxation times. In any case, the temperature dependencies determined from mechanical and dielectric spectroscopy are equivalent, as illustrated in Figure 4. The Vogel-Fulcher parameters for segmental relaxation of PI are listed in Table 1.

In the transition zone, the dynamic moduli exhibit power-law behavior over a couple decades of frequency. Although the Rouse model predicts that both  $G'(\omega)$  and  $G''(\omega)$  will vary as  $\omega'$ , experimentally this is usually observed only toward the high-frequency end of the transition zone.<sup>5</sup> The slope of the loss modulus in Figure 1 is much steeper ( $\approx 0.7$ ), comparable to values reported for polystyrene and polybutadiene.<sup>51</sup>

**Thermorheological Complexity.** The data in Table 1 indicate different temperature dependencies for the chain modes and local segmental motion. This difference should occasion a breakdown of the time-temper-

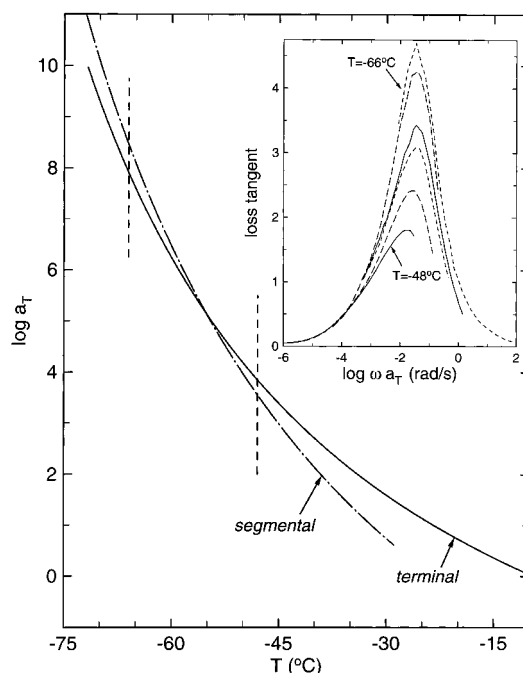


**Figure 5.** Time-temperature shift factors obtained from Figure 2 (terminal) and Figure 3 (segmental). The latter have been shifted (9.32 decades downward) to demonstrate the differing temperature dependencies. The vertical dashed lines indicate the temperature range of the loss tangent measurements shown in the inset. Note the marked thermorheological complexity in the transition zone.

ature superposition principle, notwithstanding Figure 1. This breakdown becomes evident at temperatures for which both relaxation modes contribute within the available range of experimental frequencies. This is, of course, the transition zone.

The respective shift factors for the terminal and segmental modes are plotted in Figure 5, using an expanded temperature scale to emphasize the transition region. The data for segmental relaxation has been shifted downward, making apparent its stronger temperature dependence. At these temperatures thermorheological complexity is particularly marked for the loss tangent, as shown in the inset to Figure 5.

The coupling model predicts a relationship between the temperature dependencies of different relaxations and the breadth of their respective dispersions.<sup>35-39</sup> Quantitative assessment of this prediction is possible for relaxation functions having the stretched exponential form; however, the terminal relaxation of PI deviates markedly from this shape.<sup>55</sup> Nevertheless, the qualitative prediction remains that broader dispersions will have larger time-temperature shift factors. Because segmental relaxations usually are broader than terminal dispersions, this prediction is consistent with many experimental results.<sup>39</sup>

The full width at half-maximum (fwhm) of the terminal peak in Figure 2 is 2.3 decades. Due to overlap with the transition zone, this breadth is a decreasing function of molecular weight, attaining a constant shape at sufficiently high molecular weight.<sup>46,48</sup> Consistent with such a variation with molecular weight, the breadth in the present case is  $\sim 10\%$  narrower than found for PI of  $M_w = 357\,000$ .<sup>32,33</sup> As previously noted,<sup>40</sup> the segmental relaxation function of PI is quite narrow. The fwhm of the loss modulus peak is 2 decades, decreasing with increasing temperature. Thus, PI is

unique in having a broader terminal than segmental relaxation and, according to the coupling model, differences between segmental and terminal shift factors should be quite small. This prediction differs from the results in Figure 5, where than the segmental shift factors are clearly larger.

### Summary

Mechanical and dielectric spectroscopy was carried out on high molecular weight PI. The results in the plateau zone were consistent with a relaxation spectrum having power law behavior, with an exponent approaching a previously suggested universal value. The experimentally determined values for the plateau modulus and terminal viscosity, however, were not quantitatively compatible with eq 6, derived from a power law spectrum.

Although the temperature dependence of local segmental motion was the same when measured mechanically or dielectrically, a change in the shape of the segmental relaxation function with temperature was evident. More dramatic thermorheological complexity was seen in the transition zone. Notwithstanding these results, qualitatively satisfactory master curves could be constructed, because only in the transition zone are the contributions from the chain modes and local segmental motion overlapping. Nevertheless, time-temperature extrapolation of viscoelastic properties can be subject to large errors, particularly if shift factors are determined at temperatures for which the dominant viscoelastic mode differs from the mode governing the property of interest.

The fact that the terminal and segmental dynamics have distinct temperature dependencies means that each can be associated with a different friction factor. In the tube model, however, a single local friction factor is used to describe both the chain modes and local motions; hence, the theory fails to account for thermorheological complexity in polymers. Such behavior is anticipated by the coupling model of relaxation; however, with respect to PI, the model appears to be at odds with the experimental data.

**Acknowledgment.** This work was supported by the Office of Naval Research. We thank Adel F. Halasa of the Goodyear Tire & Rubber Company for kindly preparing the polymer.

### References and Notes

- (1) de Gennes, P. G. *J. Chem. Phys.* **1971**, *55*, 572.
- (2) Doi, M.; Edwards, S. F. *The Theory of Polymer Dynamics*; Clarendon: Oxford, 1986.
- (3) Lodge, T. P.; Rotstein, N. A.; Prager, S. *Adv. Chem. Phys.* **1990**, *79*, 1.
- (4) Rouse, P. E. *J. Chem. Phys.* **1953**, *21*, 1272.
- (5) Ferry, J. D. *Viscoelastic Properties of Polymers*; Wiley: New York, 1980, Chapter 10.
- (6) Graessley, W. W. *J. Polym. Sci. Polym. Phys. Ed.* **1980**, *18*, 27.
- (7) Doi, M. In *Structure and Properties of Polymers*; Thomas, E. L., Ed.; Wiley-VCH: New York, 1993; Chapter 9.
- (8) Carreau, P. J.; De Kee, D. C. R.; Chhabra, R. P. *Rheology of Polymeric Systems*; Carl Hanser Verlag: Munich, 1997.
- (9) Rohn, C. L. *Analytical Polymer Rheology*; Carl Hanser Verlag: Munchen, 1995.
- (10) Schramm, G. *A Practical Approach to Rheology and Rheometry*; Gebreuder Haake GmbH: Karlsruhe, Germany, 1994.
- (11) Mills, N. J. *Plastics – Microstructure & Engineering Applications*, 2nd Ed.; Halsted: New York, 1993.
- (12) Ward, I. M.; Hadley, D. W. *An Introduction to the Mechanical Properties of Solid Polymers*; J. Wiley & Sons: New York, 1993.
- (13) Graessley, W. W. In *Physical Properties of Polymers*, 2nd Edition; Am. Chem. Soc.: Washington, D.C., 1993; Chapter 3.
- (14) Plazek, D. J. *J. Phys. Chem.* **1965**, *69*, 3480.
- (15) Plazek, D. J. *Polymer J.* **1980**, *12*, 43.
- (16) Ngai, K. L.; Schonhals, A.; Schlosser, E. *Macromolecules* **1992**, *25*, 4915.
- (17) Plazek, D. J.; Bero, C.; Neumeister, S.; Floudas, G.; Fytas, G.; Ngai, K. L. *Colloid. Polym. Sci.* **1994**, *272*, 1430.
- (18) Palade, L. I.; Verney, V.; Attane, P. *Macromolecules* **1995**, *28*, 7051.
- (19) Plazek, D. J.; Chay, I.-C.; Ngai, K. L.; Roland, C. M. *Macromolecules* **1995**, *28*, 6432.
- (20) Plazek, D. L.; Plazek, D. J. *Macromolecules* **1983**, *16*, 1469.
- (21) Santangelo, P. G.; Ngai, K. L.; Roland, C. M. *Macromolecules* **1996**, *29*, 3651.
- (22) Reisch, M. S. *Chem. Eng. News* **1997**, *75*, 5(36), 18.
- (23) Fetters, L. J.; Lohse, D. J.; Richter, D. Witten, T. A.; Zirkel, A. *Macromolecules* **1994**, *27*, 4639.
- (24) Colby, R. H.; Rubinstein, M.; Viovy, J. L. *Macromolecules* **1992**, *25*, 996.
- (25) Graessley, W. W.; Edwards, S. F. *Polymer* **1981**, *22*, 1329.
- (26) Roland, C. M. *Macromolecules* **1992**, *25*, 7031.
- (27) P. de Gennes, P. *J. Phys. (Paris)* **1975**, *36*, 1199.
- (28) Carella, J. M.; Gotro, J. T.; Graessley, W. W. *Macromolecules* **1986**, *19*, 659.
- (29) Graessley, W. W.; *Macromolecules* **1982**, *15*, 1164.
- (30) Fetters, L. J.; Kiss, A. D.; Pearson, D. S.; Quack, G. F.; Vitus, F. *J. Macromolecules* **1993**, *26*, 647.
- (31) Grest, G.; Fetters, L. J.; Huang, J. S., and Richter, D. In *Polymeric Systems*; Prigogine, I.; Rice, S. A., Eds.; J. Wiley: New York, 1996; Chapter 2.
- (32) Bero, C. A.; Roland, C. M. *Macromolecules* **1996**, *29*, 1562.
- (33) Roland, C. M.; Bero, C. A. *Macromolecules* **1996**, *29*, 7521.
- (34) Santangelo, P. G.; Roland, C. M. *J. Non-Crystalline Solids* **1998**, *in press*.
- (35) Ngai, K. L.; Rajagopal, A. K.; Teitler, S. *J. Chem. Phys.* **1988**, *88*, 5086.
- (36) Ngai, K. L.; Plazek, D. J. *J. Polym. Sci., Polym. Phys. Ed.* **1986**, *24*, 619.
- (37) Plazek, D. J.; Zheng, X. D.; Ngai, K. L. *Macromolecules* **1992**, *25*, 4920.
- (38) Ngai, K. L.; Plazek, D. J.; Bero, C. A. *Macromolecules* **1993**, *26*, 1065.
- (39) Ngai, K. L.; Plazek, D. J. *Rubber Chem. Technol.* **1995**, *68*, 376.
- (40) Roland, C. M.; Ngai, K. L. *Macromolecules* **1991**, *24*, 5315; **1992**, *25*, 1844.
- (41) Boese, D.; Kremer, F. *Macromolecules* **1990**, *23*, 829.
- (42) Adachi, K.; Yoshida, H.; Fukui, F.; Kotaka, T. *Macromolecules* **1990**, *23*, 3138.
- (43) Watanabe, H.; Yao, M.-L.; Osaki, K. *Macromolecules* **1997**, *30*, 997.
- (44) Okamoto, H.; Inoue, T.; Osaki, K. *J. Polym. Sci., Polym. Phys. Ed.* **1995**, *33*, 417.
- (45) Plazek, D. J. *J. Polym. Sci.; Part A-2* **1968**, *6*, 621.
- (46) Colby, R. H.; Fetters, L. J.; Funk, W. G.; Graessley, W. W. *Macromolecules* **1991**, *24*, 3873.
- (47) Gotro, J. T.; Graessley, W. W. *Macromolecules* **1984**, *17*, 2767.
- (48) Raus, V. R.; Menezes, E. V.; Marin, G.; Graessley, W. W.; Fetters, L. J. *Macromolecules* **1981**, *14*, 1668.
- (49) Baumgaertel, M.; Schausberger, A.; Winter, H. H. *Rheol. Acta* **1990**, *29*, 400.
- (50) Doi, M. *Chem. Phys. Lett.* **1974**, *26*, 269.
- (51) Jackson, J. K.; De Rosa, M. E.; Winter, H. H. *Macromolecules* **1994**, *27*, 2426.
- (52) Kannan, R. M.; Lodge, T. P. *Macromolecules* **1997**, *30*, 3694.
- (53) Jackson, J. K.; Winter, H. H. *Macromolecules* **1995**, *28*, 3146.
- (54) Colmenero, J.; Alegria, A.; Santangelo, P. G.; Ngai, K. L.; Roland, C. M. *Macromolecules* **1994**, *27*, 407.
- (55) Santangelo, P. G.; Ngai, K. L.; Roland, C. M. *Polymer* **1998**, *39*, 681.

MA971663C